Wall forces produced during ITER disruptions

H.R. Strauss[1], R. Paccagnella[2], J. Breslau[3]
[1]HRS Fusion, West Orange NJ, USA 07052
[2] Consorzio RFX and Istituto Gas Ionizzati (C.N.R), Padua, Italy
[3] Princeton Plasma Physics Laboratory, Princeton, NJ 08570
strauss@cims.nyu.edu

Abstract Nonlinear simulations with the M3D [1] code are performed of disruptions [2] produced by large scale magnetohydrodynamic (MHD) instabilities. The toroidally symmetric and asymmetric wall forces produced during a disruption are calculated in an ITER model. The disruption is produced by a vertical displacement event (VDE) and a kink mode. Expressions are derived for the wall force, including the sideways force, using a thin conducting wall model. The dependence of wall force with $\gamma\tau_w$ is obtained, where γ is the kink growth rate and τ_w is the wall penetration time. The largest force occurs with $\gamma\tau_w \approx 1$. In this regime the wall force is produced by poloidal halo current. The current and temperature quench is caused by the VDE carrying the plasma to the wall. A less resistive wall will experience less wall force.

I. Introduction

A very critical issue for the ITER device construction is to evaluate the forces produced on the surrounding conducting structures during plasma disruptions [3]. Recent studies have documented results obtained from the Joint European Torus (JET) experiment [4, 5, 6]. A major concern are non axisymmetric stresses caused by large scale MHD instabilities [7]. We extend [2] previous studies of vertical displacement events combined with disruptions [8]. In particular, here the emphasis is on the non axisymmetric wall forces. New numerical diagnostics are derived and implemented, which directly measure the forces in the resistive shell surrounding the plasma. The disruptions are simulated using the M3D [1] code. The code solves resistive MHD equations with parallel and perpendicular thermal transport. The plasma is bounded by a thin, resistive wall [9] of thickness δ. The magnetic field perturbations outside the wall are calculated with Green's functions [10, 11]. The jump in the magnetic field across the thin wall gives the wall force.

Three dimensional reduced MHD [12] simulations [13] showed that overlap of magnetic islands produced a chaotic rupturing of the magnetic field and loss of equilibrium. The magnetic field chaos causes quenching of the plasma current and pressure. This physical behavior is characteristic of a long wall penetration time, $\gamma\tau_w \gg 1$, where γ is the kink growth rate and τ_w is the wall penetration time. The present simulations are based on an ITER reference equilibrium. Disruptions were simulated by an axisymmetric vertical displacement event (VDE), along with a large scale kink instability. This is expected to be one of the worst case scenarios.

The forces and stresses on the wall are due to currents flowing in the wall that couple with the magnetic field. These currents are produced by inductive effects (eddy currents), due to time varying magnetic fluxes through the wall, and by conduction currents, generally indicated as halo currents, that can flow from the plasma to the wall. The eddy current is mainly toroidal, while the halo current is mainly poloidal. In the limit of a conducting wall, the asymmetric wall force is produced predominantly by eddy current, while for a relatively resistive wall, the asymmetric wall force is produced predominantly by halo current.

We have found that the wall force is largest in the regime $\gamma\tau_w \sim 1$, where it is predominantly due to halo current. These results were obtained in the simulations, for a given initial state, by varying the wall conductivity.

The current and temperature quench is caused by the VDE carrying the plasma to the wall. A less resistive wall will experience less wall force.

The paper is organized as follows. The resistive wall model, including the derivation of the wall force, halo current, and toroidal peaking factor (TPF), is described in section II. In section III the disruption simulations are presented, beginning with a brief description of the numerical method. Simulational results are presented, including scaling of the wall force with plasma current, halo current, and TPF. Conclusions are presented in section IV.

II. Resistive Wall Model

The plasma is bounded by a thin resistive wall of thickness δ and resistivity η_w. Surrounding this is an outer vacuum region, which can contain external current sources.

On the resistive wall boundary, integrating $\nabla \cdot \mathbf{B} = 0$ across the thin shell gives the requirement that the normal component of magnetic field is continuous at the wall,

$$B_n^v = B_n^p, \tag{1}$$

where B_n^v, B_n^p are the normal component of magnetic field in the vacuum, just outside the wall, and the plasma, just inside the wall. The normal component of the magnetic field at the wall satisfies

$$\frac{\partial B_n}{\partial t} = -\frac{\eta_w}{\delta}\nabla \cdot [\hat{\mathbf{n}} \times (\mathbf{B}^v - \mathbf{B}^p) \times \hat{\mathbf{n}}] \tag{2}$$

This gives a boundary condition to determine the vacuum field. The vacuum field is solved by the GRIN code [10]. In the wall, the current is given by

$$\mathbf{J}_w = \frac{1}{\mu_0 \delta}\hat{\mathbf{n}} \times (\mathbf{B}^v - \mathbf{B}^p). \tag{3}$$

where $\hat{\mathbf{n}}$ is the outward normal to the wall. The wall force density is $\mathbf{f}_w = \mathbf{J}_w \times \mathbf{B}_w$. Inside the wall assume that $\mathbf{B}_w = 1/2(\mathbf{B}^v + \mathbf{B}^p)$. The wall force density can be expressed

$$\mathbf{f}_w = \frac{1}{\mu_0 \delta}[B_n(\mathbf{B}^v - \mathbf{B}^p) - \frac{1}{2}(|\mathbf{B}^v|^2 - |\mathbf{B}^p|^2)\hat{\mathbf{n}})]. \tag{4}$$

The normal component has a simple physical meaning. It is the difference in magnetic pressure across the wall, divided by the wall thickness. Integrating over the wall thickness δ gives the magnetic pressure on the wall. The total wall force per toroidal angle is given by

$$\mathbf{F} = \frac{\mu_0 \delta}{2\pi R_0 L_w B_0^2} \int dl R \mathbf{f}_n. \tag{5}$$

Here the force has been normalized to be dimensionless, where B_0 is the magnetic field on axis, and $L_w = \int dl$ is the wall circumference. To obtain the dimensional force, (5) must be multiplied by $F_{dim} = 2\pi R_0 L_w B_0^2/\mu_0$. Of particular importance is the net horizontal force, F_x. Here F_x is obtained by taking the horizontal components of $\mathbf{F}$, $F_c = \int d\phi \mathbf{F} \cdot \hat{\mathbf{R}} \cos(\phi)$, $F_s = \int d\phi \mathbf{F} \cdot \hat{\mathbf{R}} \sin(\phi)$. To allow for the horizontal force to be an arbitrary direction, the horizontal force is $F_x = (F_c^2 + F_s^2)^{1/2}$. It is in units of F_{dim}.

The halo current is the poloidal current flowing into the resistive wall. Nonlinear simulations of VDEs, disruptions, and resistive wall modes with the M3D code [1] found H_f and TPF consistent with experimental data [8]. The normal component of the poloidal current integrated over the wall, I_{halo}, is

$$I_{halo}(\phi) = \frac{1}{2}\int |\hat{n} \cdot \mathbf{J}| R dl, \tag{6}$$

where dl is the length element tangent to the wall. Half the absolute value is taken in the integrand because $\nabla \cdot \mathbf{J} = 0$ implies the total normal current is zero when integrated over the wall and the toroidal angle ϕ. The toroidal peaking factor [14] is defined as the maximum of

$$\mathrm{TPF} = \frac{2\pi \mathrm{I}_{\mathrm{halo(max)}}}{\int \mathrm{I}_{\mathrm{halo}} \mathrm{d}\phi}. \tag{7}$$

In the following simulations, TPF ≈ 2. The ratio of halo current to total plasma current is also important. The halo current fraction H_f is defined as the ratio

$$H_f = \frac{\int I_{halo} d\phi}{I_\phi}, \tag{8}$$

where the toroidal current is $I_\phi = \int J_\phi dR dZ$, and the initial value of I_ϕ is used.

III. Disruption Simulation

The M3D extended MHD code [1] solves the full resistive MHD equations. The open field line region surrounding the plasma is treated as a resistive MHD vacuum with very large resistivity, small density, and low temperature. A resistive wall with the shape of the experimental vacuum vessel, slightly smoothed, bounds the vacuum. The code does not assume large aspect ratio or incompressibility and it keeps the full plasma X-point geometry. The plasma velocity is evolved self-consistently, by solving the MHD momentum evolution equations.

A single, scalar temperature is assumed, with the ion and electron temperatures taken to be proportional. Temperature evolution includes parallel[15] and perpendicular thermal transport. The effective parallel thermal diffusion coefficient is $\kappa_\parallel = 2Rv_A$, much larger than the perpendicular diffusion, where R is the major radius and v_A is the Alfvén speed. The resistivity varies as $T^{-3/2}$ self-consistently, where T is the temperature. Spatially constant perpendicular thermal conductivity $\kappa_\perp$ and viscosity $\mu_\perp$ were employed.

M3D uses an unstructured mesh [16] with a finite element discretization in the poloidal, (R, Z) plane. In the toroidal direction, a uniform mesh in toroidal angle ϕ is used, with a pseudospectral discretization. The mesh boundary is treated as a thin resistive wall. Outside the resistive wall is the vacuum region.

In the following, M3D is used to calculate a disruption. The initial state is an ITER reference equilibrium, FEAT15MA, written to a file in EQDSK [17] format. This was read into M3D and used to generate a mesh and initialize a nonlinear simulation. The initial equilibrium had $q = 1.1$ on axis.

In the simulation the Lundquist number was chosen to be $S = 10^5$ on axis and $S = 10^2$ at the wall. The Lundquist number must be much lower than experiment for numerical reasons. The wall resistivity η_w divided by wall thickness, was chosen to have a range of values. In the following example of Fig.1, $\tau_w = 10R/v_A$, where $\tau_w = \delta a/\eta_w$, with δ the wall thickness and a the effective minor radius, and $\tau_A = R/v_A$ is the toroidal Alfvén time. The perpendicular thermal diffusivity was $\kappa_\perp = 10^{-5}\epsilon a v_A$, and the viscous diffusivity was $\mu_\perp = 10^{-4}\epsilon a v_A$, where $\epsilon = a/R$.

The velocity boundary condition was $v_n = 0$. The magnetic field boundary condition was given by (2).

The initial equilibrium is VDE unstable. The equilibrium was made to be kink unstable by rescaling. The initial equilibrium had $q_0 = 1.1$, and initial total current I_0. The equilibrium was rescaled to generate equilibria with $q < 1$ on axis, and $1 < I/I_0$. The poloidal magnetic field and toroidal current were rescaled by multiplying by a rescaling

parameter, and the pressure was rescaled by the square of the rescaling parameter. Such a state might be produced during a VDE, as current is scraped off by wall interaction.

The following example was produced by first evolving a VDE, then adding a kink perturbation as the plasma approached the wall. The wall resistivity for this example had $\gamma\tau_w \approx 1$, and the current enhancement was $I/I_0 = 1.6$. The contours are all shown in the poloidal plane (R, Z) with toroidal angle $\phi = 0$.

In Fig.1, at time $t = 38.54\tau_A$, the VDE and kink mode have developed nonlinearly, with the plasma in contact with the wall. Fig.1(a) shows the poloidal magnetic flux penetrating the wall. Fig.1(b) shows the toroidal current. Much of the bulk toroidal plasma current has decayed. The current is concentrated in intense filaments localized at the magnetic o - point and x - point of Fig.1(a). The toroidal flux RB_ϕ in Fig.1(c) has a large poloidal variation at the wall, indicating a large halo current.

The time history of the normalized total pressure P, total toroidal current I_p, horizontal force F_x, halo current fraction H_f, and toroidal peaking factor TPF, are shown in Fig.2. The quantities I, P, and F_x are in arbitrary units. The TPF peaks first, reaching a value of about 2.2. Next the pressure quench begins, closely followed by the current. The pressure quench and current quench are almost simultaneous because the pressure and current are carried the wall by the VDE. The halo current fraction H_f peaks during the current quench. The horizontal wall force F_x is closely correlated in time with the halo current fraction H_f. This indicates a strong causal connection of the wall force and the halo current.

The scaling of wall force with wall resistivity was obtained for the same initial states with a VDE as above, by varying τ_w. The results are shown in Fig.3. The two curves labeled "1" and "2" connect computed values, for two rescalings of the initial equilibrium. The point marked "a" on the upper curve "1" corresponds to the simulations presented above. The second set of simulations on curve "2" correspond to a less unstable rescaling of the initial state, with $I/I_0 = 1.28$, which is more realistic. The maximum force in all cases occurs when $\gamma\tau_w \approx 1$. When $\gamma\tau_w \gg 1$, the wall is a good conductor, and induced (eddy) wall current predominantly produces the wall force. In the case $\gamma\tau_w \sim 1$, there is significant magnetic flux penetration through the wall, and the wall force is much larger. The force in this regime is produced predominantly by halo current.

In terms of ITER parameters, the toroidal field is $B_\phi = 5.3T$, producing a magnetic pressure of $2.24 \times 10^7 N/m^2$. Multiplying by the plasma surface area $2\pi \int dlR = 804m^2$ gives the total wall force in ITER $F_{dim}^{ITER} = 1.81 \times 10^{10} N$. The horizontal wall force is $F_x \times F_{dim}$. In ITER terms, the peak sideways force, marked "b" in Fig.3, for the less unstable case "2", that we consider more realistic, is $F_x^{ITER} = F_x \times F_{dim}^{ITER} = 70MN$. This is somewhat more than the predicted value used in the ITER design [18]. The total wall force F_{dim} scales as I_p^2, where $I_p \propto Ba$ is the plasma current, assuming fixed aspect ratio and q. The ITER current is about 5 times greater than the JET current, so that the JET horizontal force in this particular case would be about 2.75 MN. This value is consistent with experiments [6].

In JET [7, 19], the quantity $dI_\phi/d\phi$ was measured, where I_ϕ is the toroidal plasma current as a function of toroidal angle, and was compared to the $dM_{IZ}/d\phi$, where $M_{IZ} = \int J_\phi Z dR dZ$ is the of the vertical moment of the toroidal current density. The current was measured in disruptions in which there was usually an upward VDE, and occasionally a downward VDE. The net toroidal variation of I_ϕ is here not caused by Hiro current flowing into the wall [7], but by the vertical asymmetry produced by the VDE displacement [2]. The variation of the toroidal current is accompanied by halo current to the wall, from

$\nabla \cdot J = 0$. Fig.4 shows time history of $CY = C(I_\phi, M_{IZ})$, for the case of Figs. 1 - 2, where $C(a,b) = (\int d\phi ab)(\int d\phi a^2)^{-1/2}(\int d\phi b^2)^{-1/2}$. The correlation is positive, and coincides with the halo current. Also shown are the correlations $FX = C(F_R, \xi_R)$ and $FY = C(F_Z, \xi_Z)$, where F_R, F_Z are components of the force and ξ_R, ξ_Z are the plasma displacements in the $\hat{R}, \hat{Z}$ directions, integrated over the poloidal plane. The force is positively correlated with the plasma displacement.

IV. Discussion and conclusion

The toroidally symmetric and asymmetric wall forces produced during a disruption are calculated in an ITER model. A new method is derived for calculating wall forces directly from magnetic field pressure at a resistive wall. Simulations were done with M3D using an ITER reference equilibrium, modified so that it was both VDE and kink unstable. An example was chosen in which a VDE carried the plasma close to the wall, when it became kink unstable. The simulations show that the pressure, current and wall force are quenched by the contact of the plasma with the wall. We remark that the VDE kink simulation that we have presented so far is not fully self-consistent. In fact, the plasma edge should be scraped off or cooled by the plasma wall interaction. This should cause the current channel to shrink, and the current density to increase, so that q on axis will decrease in time. This will in turn enhance plasma instability and trigger the kink mode. In the simulation presented here, the current is rescaled initially. A completely self consistent treatment will require additional physics modeling of the plasma wall interaction.

The dependence of wall force on wall resistivity was studied. It was found that the relative importance of eddy current and halo current on the sideways wall force depends strongly on $\gamma\tau_w$. If the wall is a relatively good conductor, such that $\gamma\tau_w \gg 1$, the eddy current predominates in producing the wall force, and the wall resistivity has little effect. In the case, $\gamma\tau_w \approx 1$, the halo current predominates, and the wall force is much larger. For a given $\gamma\tau_w$, Fig.3 shows that a less unstable plasma will produce less wall force.

The variation of the horizontal force with wall resistivity which was observed in the simulations of Fig.3 offers an important opportunity to ameliorate the sideways force of disruptions. If the wall can be made more conducting, it is possible to reduce the wall force by a large factor. The JET experiment operates in a regime with large halo currents relative to eddy currents, which is the regime $\gamma\tau_w \sim 1$. Results in this regime may overestimate the forces on a better conducting wall. However it should be noted that, due to axisymmetric vertical control, it is in general difficult in any magnetic confinement device to operate with a very conducting wall, which will shield the vertical field penetration. Moreover, the very complicated structure of the ITER wall, where many cuts and holes in the metal wall and blanket modules are present, will certainly make more difficult to fulfill this requirement.

In conclusion, in this paper we have presented a self consistent computational model for 3D MHD disruption simulations. Within this model we calculated the wall forces, with particular emphasis on the non axisymmetric sideways force. We gave an example for ITER with a force in the range of 70 MN, a value which can vary widely with the growth rate γ and the wall resistivity τ_w.

Our model is not completely self-consistent, especially in the modeling of the self-adjustment of the current profile, due to plasma wall interaction and plasma cooling. Future work will be necessary to carry out more self consistent simulations, as well as to compare simulation results with experimental data from JET and other tokamaks.

Acknowledgments

This work was supported in part (H.S. and J.B.) by the U.S.D.O.E and in part (R.P.)

by EFDA.

References

[1] PARK, W., BELOVA, E.V., FU, G.Y., TANG, X., STRAUSS, H. R., SUGIYAMA, L.E. Phys. Plasmas **6** (1999) 1796 (1999).

[2] STRAUSS, H. R., PACCAGNELLA, R., BRESLAU, J. Phys. Plasmas **17** (2010) 082505.

[3] HENDER, T., WESLEY, J. C., BIALEK, J. *et al.,* Nuclear Fusion **47** (2007) S128 - 202.

[4] RICCARDO, V, ARNOUX, G, BEAUMONT, P., *et al.,* Nuclear Fusion **49** (2009) 055012 (2009).

[5] RICCARDO, V., HENDER, T. C., LOMAS, P. J., *et al.,* Plasma Phys. Control. Fusion **46** (2004) 925.

[6] RICCARDO, V., NOLL. P., WALKER, S. P., Nucl. Fusion (2000) **40** 1805.

[7] ZAKHAROV, L. E., Phys. Plasmas (2008) **15** 062507.

[8] PACCAGNELLA, R., STRAUSS, H. R., BRESLAU, J., Nucl. Fusion (2009) **49** 035003.

[9] STRAUSS, H. R., Computer Physics Communications 164, (2004) 40.

[10] PLETZER, A., Dr. Dobb's Journal **334** (2002) 36,
http://ellipt2d.sourceforge.net

[11] CHANCE, M., Phys. Plasmas **4** (1997) 2161.

[12] STRAUSS, H. R., Phys. Fluids **19** (1976) 134.

[13] WADDELL, B. V., CARRERAS, B., HICKS, H. R., HOLMES, J. A., LEE, D. K., Phys. Rev. Lett. **41** (1978) 1386.

[14] POMPHREY, N., BIALEK, J., PARK, W., Nuclear Fusion 38 (1998) 449.

[15] PARK, W., MONTICELLO, D., STRAUSS, H., MANICKAM, J., Phys. Fluids **2**9 (1986) 1171.

[16] STRAUSS, H. R., LONGCOPE, W., J. Comput. Phys. 147 (1998) 318 - 336.

[17] LAO, L.L., ST. JOHH, H., STAMBAUGH, R.D., *et al., et al.*, Nucl. Fusion **25** (1985) 1611.

[18] IOKI, K., BACHMANN, C., CHAPPUIS, P., *et al.,* Fusion Engineering and Design **84** (2009) 229.

[19] GERASIMOV, S. N., HENDER, T. S., JOHNSON, M. F., ZAKHAROV, L. E., *et al.,* Scaling JET disruption sideways forces to ITER, Proc. of EPS 37th Conference on Plasma Physics, Dublin, Ireland (2010).

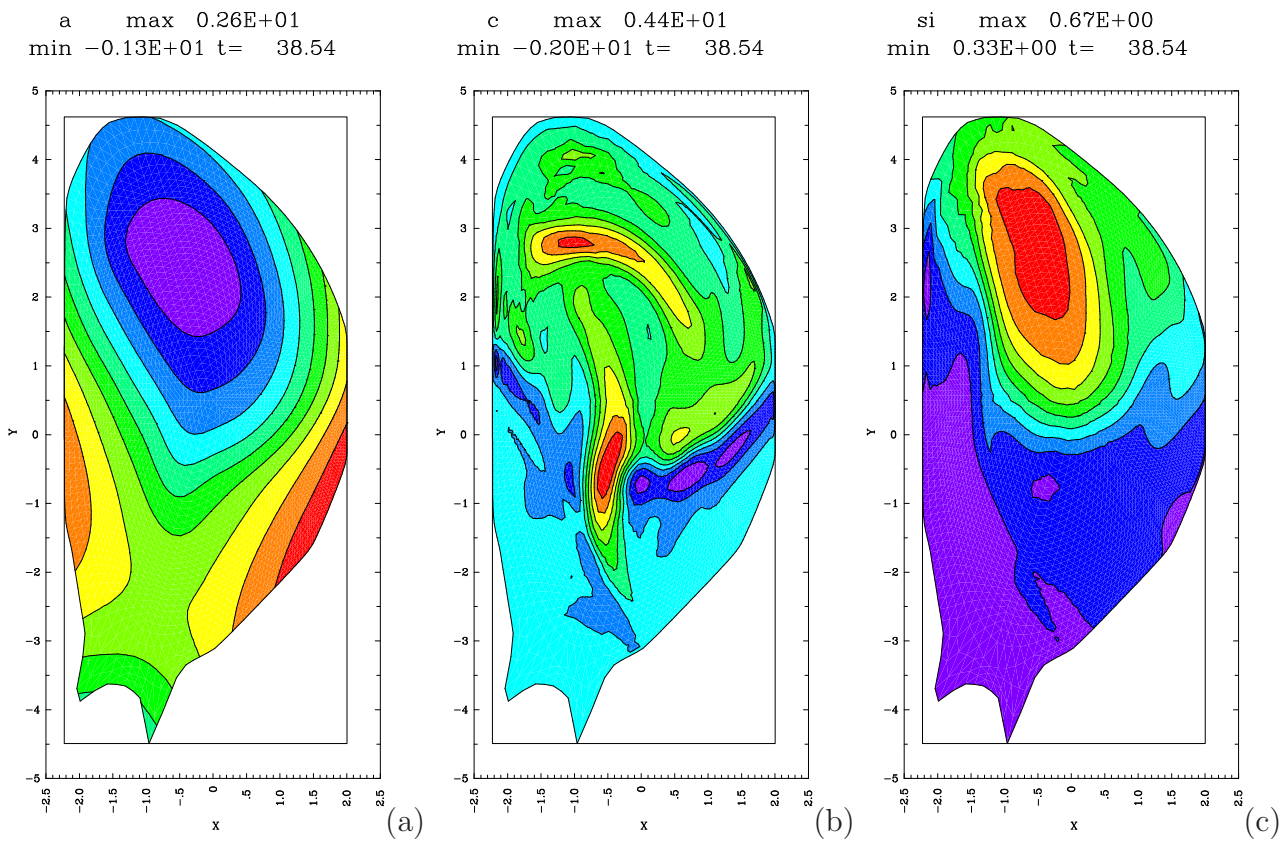

Figure 1: *(a) poloidal flux ψ, (b) toroidal current $-RJ_\phi$, (c) toroidal field RB_ϕ , at $t = 38.54\tau_A$, with toroidal angle $\phi = \pi$.*

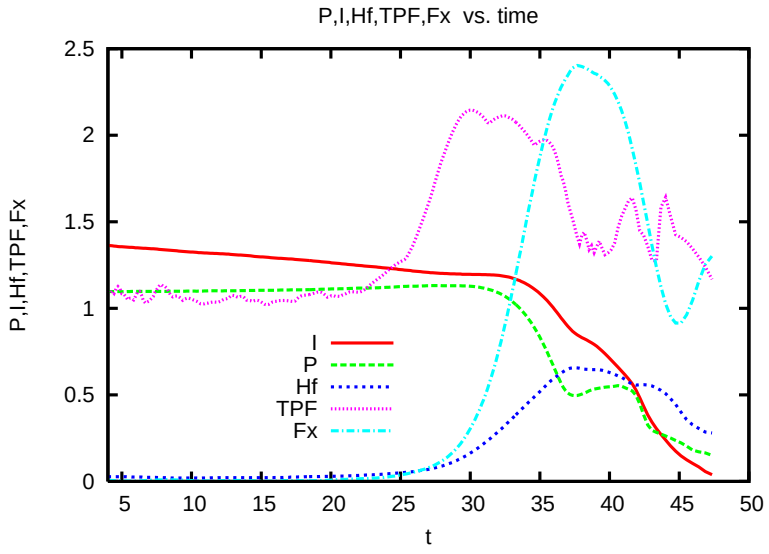

Figure 2: *(a) toroidal current I, pressure P, TPF, halo current fraction H_f and horizontal force F_x as a function of time. The quantities I, P, and F_x are in arbitrary units. There is a close time correlation of halo current fraction H_f and horizontal force F_x.*

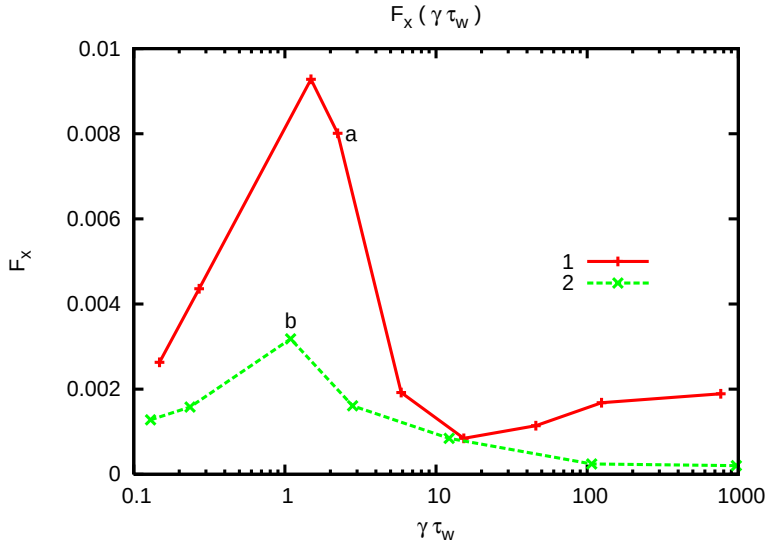

Figure 3: *Scaling of horizontal F_x, with $\gamma\tau_w$. The force tends to a limit for an ideal conducting wall $\gamma\tau_w \to \infty$. The force has a maximum for $\gamma\tau_w \approx 1$. The curves labeled "1" and "2" correspond to different initial current rescaling. The previous figures correspond to point "a" on curve "1." The lower curve "2", which corresponds to more stable initial states, is more realistic.*

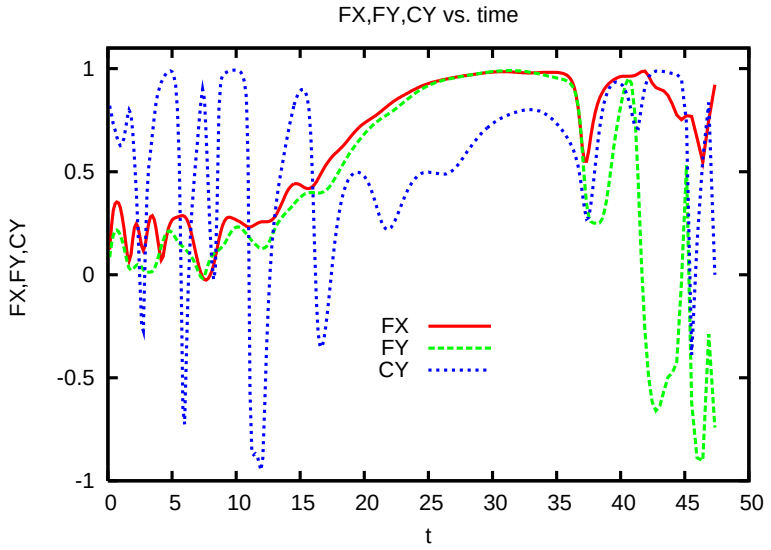

Figure 4: *Correlations as a function of time. The correlations change sign after F_x is quenched.*